

Electronic structure and magnetic anisotropy for nickel-based molecular magnets

Kyungwha Park^{1,2,*}, En-Che Yang³, and David N. Hendrickson³

¹*Center for Computational Materials Science, Code 6390,
Naval Research Laboratory, Washington DC 20375*

²*Department of Physics, Georgetown University, Washington DC 200057*

³*Department of Chemistry, University of California at San Diego, La Jolla, CA 92093-0358*

(Dated: October 25, 2018)

Recent magnetic measurements on tetra-nickel molecular magnets $[\text{Ni}(\text{hmp})(\text{ROH})\text{Cl}]_4$, where $\text{R}=\text{CH}_3$, CH_2CH_3 , or $(\text{CH}_2)_2\text{C}(\text{CH}_3)_3$ and hmp^- is the monoanion of 2-hydroxymethylpyridine, revealed a strong exchange bias prior to the external magnetic field reversal as well as anomalies in electron paramagnetic resonance peaks at low temperatures. To understand the exchange bias and observed anomalies, we calculate the electronic structure and magnetic properties for the Ni_4 molecules with the three different ligands, employing density-functional theory. Considering the optimized structure with possible collinear spin configurations, we determine a total spin of the lowest-energy state to be $S = 0$, which does not agree with experiment. We also calculate magnetic anisotropy barriers for all three types of Ni_4 molecules to be in the range of 4-6 K.

PACS numbers: 75.50.Xx, 73.22.-f, 75.30.Gw, 71.15.Mb

Molecular magnets have received much attention in the past decade because of observed quantum features at the mesoscopic level and potential utilization as ultra-high density information storage devices or magnetic sensors. The first prototype molecular magnet is $\text{Mn}_{12}\text{O}_{12}(\text{CH}_3\text{COO})_{16}(\text{H}_2\text{O})_4$ (hereafter Mn_{12} -acetate),¹ which has a total ground-state spin of $S = 10$ and magnetic anisotropy barrier of 65 K.^{2,3} Magnetic hysteresis loop measurements on Mn_{12} -acetate showed quantum tunneling of magnetic moment through the magnetic anisotropy barrier when the external magnetic field was applied along the easy axis.³

Recently molecular magnets $[\text{Ni}(\text{hmp})(\text{ROH})\text{Cl}]_4$ (hereafter Ni_4) were synthesized,⁴ where $\text{R}=\text{CH}_3$, CH_2CH_3 , or $(\text{CH}_2)_2\text{C}(\text{CH}_3)_3$ (abbreviated to Me, Et, and tBuEt, respectively). They revealed qualitatively different tunneling features from the typical molecular magnets such as Mn_{12} -acetate. For Ni_4 , the tunneling was observed prior to magnetic field reversal but no tunneling in zero magnetic field.⁴ The similar behavior has been observed in a dimeric form of the molecular magnet $[\text{Mn}_4\text{O}_3\text{Cl}_4(\text{O}_2\text{CET})_3(\text{NC}_5\text{H}_5)_3]_2$ (hereafter Mn_4).^{5,6} Additionally, electron paramagnetic resonance (EPR) spectra on Ni_4 exhibited unusual double sets of low-temperature peaks corresponding to somewhat different values of magnetic anisotropy barriers.⁷ This anomaly in the EPR spectra has never been reported from any other kinds of molecular magnets including the Mn_4 dimer. Each Ni_4 molecule comprises four Ni^{2+} ($S_i = 1$) ions located at the corners of a slightly distorted cube and coupled through oxygen anions with S_4 symmetry shown in Fig. 1. Unlike Mn_{12} -acetate and Mn_4 dimer, the Ni_4 molecular magnets are not well separated from each other so that there are four interacting nearest neighboring molecules.⁴ The intermolecular interactions can be tailored by different sizes of ligands such as MeOH, EtOH, and tBuEtOH. Among the three different types of Ni_4 , the MeOH and EtOH

complexes consist of two sublattices, each of which is an inter-penetrating diamond lattice.⁴

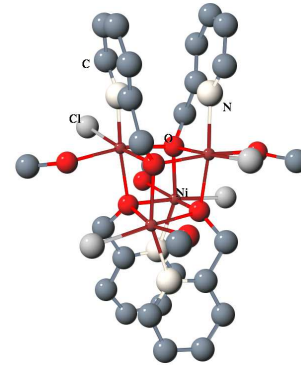


FIG. 1: Geometry of molecule magnet $[\text{Ni}(\text{hmp})(\text{MeOH})\text{Cl}]_4$. For simplicity, hydrogen atoms are not shown.

In this paper, as an attempt to better understand the observed tunneling aspects and EPR spectra, preliminary first-principle calculations on the Ni_4 molecular magnets will be presented with the three different ligands using density-functional theory (DFT). Geometries of the Ni_4 molecular magnets with the different ligands will be relaxed and electronic density of states will be discussed along with ground-state magnetic moments and magnetic anisotropy. All of our calculated results will be compared with available experimental data.

Density-functional calculations⁸ were performed with spin-polarized all-electron Gaussian-orbital basis sets and the generalized-gradient approximation (GGA).⁹ For this purpose, the Naval Research Laboratory Molecular Orbital Library (NRLMOL)¹⁰ is used. Compared to Mn_{12} -acetate and Mn_4 dimers, the Ni_4 molecular magnets need much finer mesh for faster convergence of total energy. Five different Ni_4 molecules are taken into account in density-functional calculations: a tBuEtOH complex and two crystallographically inequivalent molecules of

TABLE I: Calculated energies (in units of eV) of different collinear spin configurations relative to the lowest-energy configuration ($M_s = 0$) for the three types of Ni_4 . Here MeOH.01 represents a molecule belonging to the first sublattice of the MeOH complex.

	$E(M_s = 4)$	$E(M_s = 2)$	$E(M_s = 0)$
MeOH.01	0.0308	0.0023	0.0000
EtOH.01	0.0289	0.0042	0.0000
tBuEtOH	0.0283	0.0056	0.0000

TABLE II: Magnetic moments captured by spheres around ions in units of μ_B for $M_s = 4$ of the EtOH complex and for $M_s = 10$ of the Mn_{12} -acetate. For Ni_4 , O(b) denotes a bridging oxygen and O(l) represents a dangling oxygen from the cube. For Mn_{12} -acetate, O(1) [O(2)] bridges Mn^{4+} (1) [Mn^{3+} (2)] ions.

Ni	Cl	O(b)	O(l)	N	
1.57	0.053	0.166	0.043	0.049	
Mn^{4+} (1)	Mn^{3+} (2)	Mn^{3+} (3)	O(1)	O(2)	O(3)
-2.58	3.62	3.55	0.012	-0.024	-0.029

the MeOH and EtOH complexes. For each molecule, a relaxed geometry is found starting from a ferromagnetic $M_s = 4$ spin configuration until forces exerted on any atom become relatively small (where $2M_s$ is magnetic moment). Although the moment is not fixed during self-consistent iterations, it converges to $M_s = 4$. With the relaxed geometry, two other collinear spin configurations, $M_s = 2$ and $M_s = 0$, are considered as starting magnetic moments to calculate energies and compare to the energy of $M_s = 4$. As shown in Table I, for the MeOH, EtOH, and tBuEtOH complexes, the $M_s = 0$ configuration has the lowest energy. This is in contrast to the experimental result^{4,7} which exhibited a ferromagnetic coupling $S = 4$ as the ground state for all five Ni_4 molecules. Even though not shown in Table I, there are no differences in total moments of the ground states for the two inequivalent molecules of the MeOH and EtOH complexes. An experiment on a tetra-nickel-based molecular magnet within a Mo_{12} cage, $[\text{Mo}_{12}\text{O}_{30}(\mu_2\text{-OH})_{10}\text{H}_2\{\text{Ni}(\text{H}_2\text{O})_2\}_4]$, however, revealed that the ground state has a total spin of $S = 0$.¹¹ The experimental finding of the ground-state spin was confirmed by density-functional calculations carried out by Postnikov *et al.*¹² In this system, two Ni ions are bridged via O- Mo_2 -O, while in our system Ni ions are bridged via oxygen anions only.

To investigate what may cause the discrepancy between theory and experiment, we calculate the magnetic moment captured by each atom, the electronic density of states projected on individual atom, and the spin-flip energy gaps for the $M_s = 4$ configuration. Within a sphere

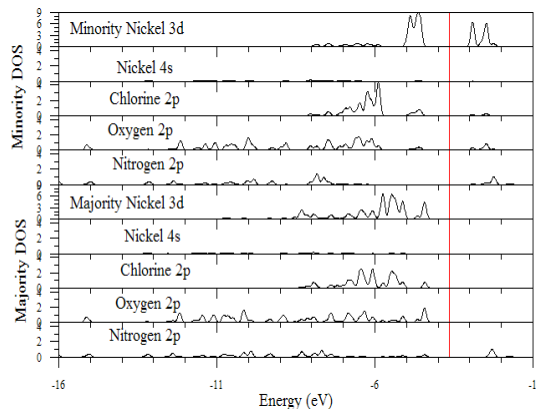


FIG. 2: Electronic majority- and minority-spin density of states (DOS) projected onto Ni(3d), Ni(4s), Cl(2p), O(2p), and N(2p) of $[\text{Ni}(\text{hmp})(\text{EtOH})\text{Cl}]_4$. All projected DOS have the same scale except for Ni(3d) DOS. The vertical line denotes the Fermi level.

of 2.3 bohr radius around a Ni ion, a moment of $1.6\mu_B$ is found. The second dominant contribution to the total moment arises from oxygen anions bridging Ni ions in the cube. A moment of $0.17\mu_B$ is found within a sphere of 1.2 bohr radius around one of the oxygen anions. This is approximately 10% of the captured moment around the Ni ion. Compared to a ferrimagnetic structure of the Mn_{12} -acetate and Mn_4 monomer,^{13,14,15,16} somewhat larger moments are found around the oxygen anions in Ni_4 (Table II). Interestingly, for the $M_s = 0$ configuration, a bridging O anion in Ni_4 bears a moment of $0.073\mu_B$ within a sphere of 1.2 bohr radius. From the calculated electronic density of states (Fig. 2) projected onto Ni 3d orbitals for $M_s = 4$, we find that most of the electron spin density is localized at the Ni sites. Notice that some of the oxygen 2p orbitals for minority spin are not occupied, although all majority-spin O 2p orbitals are occupied. This might imply a possible small leakage of spin density to the O sites. However, more scrutinized studies are required to conclude that this, in fact, attributes to the antiferromagnetic coupling in the calculated lowest-energy state. Another intriguing point is that as shown in Table I, collinear spin excitations for Ni_4 have an order of magnitude lower energies than those for the Mn_{12} -acetate¹⁴ and Mn_4 monomer^{15,16}. A majority-minority spin-flip gap ranges from 1.4 eV to 1.6 eV and a minority-majority spin-flip gap varies between 1.8 eV and 2.1 eV depending on ligands as shown in Table III. It seems that the $M_s = 4$ configuration appears to be magnetically stable since the spin-flip gaps are much larger than thermal energy.

An expectation value of the orbital angular momentum in the ground state of molecular magnets is typically quenched so that the ground-state spin manifold has a $(2S + 1)$ -fold degeneracy. The degeneracy can be lifted by spin-orbit coupling, which leads to magnetic anisotropy in the system. A generalized second-order

TABLE III: Majority LUMO(lowest unoccupied molecular orbital)- HOMO(highest occupied molecular orbital) gaps, minority LUMO-majority HOMO gaps, majority LUMO-minority HOMO gaps, minority HOMO-LUMO gaps in units of eV, and magnetic anisotropy barriers (MAB) in units of kelvin for $M_s = 4$ of the three types of Ni_4 .

	Mj L-H	Mn L-Mj H	Mj L-Mn H	Mn L-H	MAB
MeOH.01	1.74	1.38	1.83	1.47	4.4
EtOH.01	2.02	1.47	2.18	1.62	5.9
tBuEtOH	1.97	1.57	2.12	1.71	5.4

single-spin Hamiltonian is given by

$$\mathcal{H} = -DS_z^2 + E(S_x^2 - S_y^2) \quad (1)$$

where z is the easy axis, D is the uniaxial anisotropy parameter, and E is the transverse anisotropy parameter. To calculate the energy shift of the ground state, we consider the spin-orbit coupling as a small perturbation and use the computed single-electron orbitals and orbital energies¹³ for the relaxed $M_s = 4$ geometry. Because of S_4 symmetry of the Ni_4 molecule, the first term in Eq. (1) only survives. Calculated magnetic anisotropy barriers ($= DM_s^2$) for all five different Ni_4 molecules are in the range of 4-6 K so that $D = 0.25 - 0.37$ K. See Table III. Measured EPR spectra on the five Ni_4 molecules revealed that values of D are in the range of 0.72-1.03 K and that the two inequivalent molecules of the MeOH and EtOH complexes have considerably different values of D .⁷ The calculated values of D are merely 36% of the

experimentally extracted values. Numerical uncertainties in density-functional calculations prevent from differentiating between the anisotropy barriers of the two inequivalent molecules of the MeOH and EtOH complexes or between the barriers of the Ni_4 molecules with different ligands. A single-ion anisotropy projected^{14,17} onto a Ni ion in the MeOH complex provides local $D = 1.52$ K and local $E = 0.47$ K. The local easy axis of the Ni ion is found to be tilted by 10.5° from the global easy axis. Due to lack of Jahn-Teller distortion, a small value of the local D is theoretically expected for Ni^{2+} ions.

In summary, we have considered the Ni_4 molecular magnets with three different ligands in volume and carried out first-principle calculations of the electronic and magnetic structure. We found that the calculated lowest-energy state has a total spin of $S = 0$, although experimental data indicated $S = 4$. This is quite unusual because density-functional theory, so far, predicted/confirmed correct ground-state spins for a variety of molecular magnets such as the Mn_{12} -acetate^{13,14}, Mn_4 monomer^{15,16}, Co_4 molecule¹⁷, and Fe_4 molecule¹⁸. Although the reason has not yet been clarified, our preliminary studies tentatively suggested a plausible incomplete localization of spin density on Ni ions. There were no prominent effects of the ligands in different volume on the electronic structure and magnetic anisotropy of the Ni_4 molecules.

K.P. is grateful to M. R. Pederson and S. Hill for helpful discussion. K.P. was supported in part by ONR and the DoD HPCMO CHSSI program. E.-C.Y. and D.N.H. were supported by NSF Grants Nos. CHE-0123603, CHE-0350615, and DMR-0103290.

* Electronic address: park@dave.nrl.navy.mil

¹ T. Lis, Acta Crystallogr. B **36**, 2042 (1980).

² R. Sessoli, D. Gatteschi, A. Caneschi, and M.A. Novak, Nature (London) **365**, 141 (1993)

³ J. R. Friedman, M. P. Sarachik, J. Tejada, and R. Ziolo, Phys. Rev. Lett. **76**, 3830 (1996); L. Thomas, F. Lioni, F. R. Ballou, D. Gatteschi, R. Sessoli, and B. Barbara, Nature(London) **383**, 145 (1996).

⁴ E.-C. Yang, W. Wernsdorfer, S. Hill, R. S. Edwards, M. Nakano, S. Maccagnano, L. N. Zakharov, A. L. Rheingold, G. Christou, and D. N. Hendrickson, Polyhedron **22** 1727 (2003).

⁵ D. N. Hendrickson, G. Christou, E. A. Schmitt, E. Libby, J. S. Bashkin, S. Wang, H. -L. Tsai, J. B. Vincent, P. D. W. Boyd, J. C. Huffman, K. Folting, Q. Li, and W. E. Streib, J. Am. Chem. Soc. **114**, 2455 (1992).

⁶ W. Wernsdorfer, N. Aliaga-Alcade, D. N. Hendrickson, and G. Christou, Nature, **416** 406 (2002).

⁷ R. S. Edwards, S. Maccagnano, E.-C. Yang, S. Hill, W. Wernsdorfer, D. N. Hendrickson, and G. Christou, Polyhedron **93**, 7807 (2003).

⁸ W. Kohn and L. J. Sham, Phy. Rev. **140**, A1133 (1965).

⁹ J. P. Perdew, K. Burke, and M. Ernzerhof, Phys. Rev.

Let. **77**, 3865 (1996).

¹⁰ M. R. Pederson and K. A. Jackson, Phy. Rev. B **41**, 7453 (1990); K. A. Jackson and M. R. Pederson, *ibid.* **42**, 3276 (1990); D. V. Porezag, Ph.D. thesis, Chemnitz Technical Institute, 1997.

¹¹ A. Müller, C. Beugholt, P. Kögerler, H. Bögge, S. Bud'ko, and M. Luban, Inorg. Chem. **39**, 5176 (2000).

¹² A. V. Postnikov, M. Brüger, and J. Schnack, preprint cond-mat/0404343 (unpublished).

¹³ M. R. Pederson and S. N. Khanna, Phys. Rev. B **60**, 9566 (1999).

¹⁴ K. Park, M. R. Pederson, and C. S. Hellberg, Phys. Rev. B **69**, 014416 (2004).

¹⁵ K. Park, M. R. Pederson, S. L. Richardson, N. Aliaga-Alcalde, and G. Christou, Phys. Rev. B **68**, 020405(R) (2003).

¹⁶ K. Park, M. R. Pederson, and N. Bernstein, J. Phys. Chem. Sol. **65**, 805 (2004).

¹⁷ T. Baruah and M. R. Pederson, Chem. Phys. Lett. **360**, 144 (2002).

¹⁸ J. Kortus J, M. R. Pederson, T. Baruah, N. Bernstein, C. S. Hellberg, Polyhedron **22**, 1871 (2003).